Flexural to shear and crushing failure transitions in RC beams by the bridged crack model

A. Carpinteri & G. Ventura
Politecnico di Torino, Torino, Italy

J. R. Carmona
Universidad de Castilla-La Mancha, Ciudad Real, Spain

ABSTRACT: The *bridged crack model* has been developed for modelling the flexural behaviour of reinforced concrete beams and related size effects explaining brittle-ductile-brittle failure mode transitions. In the present paper the model is extended to analyze shear cracks and concrete crushing, introducing a given shape for the hypothetical crack trajectory and determining the initial crack position and the load versus crack length curve for three point bending problems. The proposed formulation reproduces the pure Mode I flexural behaviour as a particular case, so that the flexural and the diagonal tension (shear) failures modes can be immediately compared to detect which one dominates and determine the relevant failure load. A concrete crushing criterion completes the model. All the mutual transitions between the different collapse mechanisms can be predicted. In the paper these transitions are shown by varying the governing nondimensional parameters.

1 INTRODUCTION

For a long time, the transitions between flexural and diagonal tension failures in reinforced concrete elements —inside a consistent theoretical framework— have represented an unsolved problem. The main issue for the present analysis is to get a consistent modelling of shear cracks behavior and diagonal tension failure as well as concrete crushing mechanisms. These problems, despite numerous extensive studies over the past 50 years, still remain unsolved for a completely satisfying framework, unifying all the failure modes, so that a direct relation between failure mode transition could be drawn.

Shear crack propagation and diagonal tension failure have been addressed in the literature by several authors with different approaches. In the field of Fracture Mechanics and using a cohesive model to describe concrete behaviour, some analyses have been performed by Gustafson and Hillerborg (Gustafsson and Hillerborg 1983) and Niwa (Niwa 1997) among others. In the framework of Linear Elastic Fracture Mechanics and in order to avoid finite element computations, some models are especially remarkable in the long list of literature contributions. In particular, Jenq and Shah (Jenq and Shah 1989) analysed the diagonal shear fracture superposing the contribution of concrete and steel bars, with a technique that is somehow conceptually close to the *bridged crack model* (Carpinteri 1984). Some further development of this work with other original contributions were made by So and Karihaloo (So and Karihaloo 1993).

The *bridged crack model* has been originally proposed by Carpinteri (Carpinteri 1981; 1984) for the study of reinforced concrete beams by Fracture Mechanics. The problem of the size effect and the brittle-ductile transition were analyzed with reference to the problem of minimum reinforcement (Carpinteri et al. 1999; Bosco and Carpinteri 1992). Subsequently, the action of cohesive stresses has been introduced in addition to that of the reinforcing bars (Carpinteri et al. 2003). More recently, the model has been further extended analysing concrete crushing by Fracture Mechanics concepts (Carpinteri et al. 2004) and leading to analyse in a consistent way the interaction between flexural (yielding) and crushing failures. Moreover, while limit state analysis yields only the ultimate load, the *bridged crack model* reveals in addition scale effects, instability phenomena and brittle-ductile failure transition of the structural member.

In the present work, the behaviour of reinforced concrete beams without stirrups is analyzed, using the *bridged crack model*. To extend the model to account for the shear cracks behavior and to evaluate diagonal tension failure load, some additional hypotheses about the crack trajectory and for the evaluation of the stress-intensity factors are assumed. In this way the different collapse modes are joined together into a unified general model, so that the simulation of the transitional phenomena is naturally accomplished. The model is analysed showing the influence of the variation in the nondimensional parameters on the mechanical response of the reinforced concrete element and the related failure mode transitions.

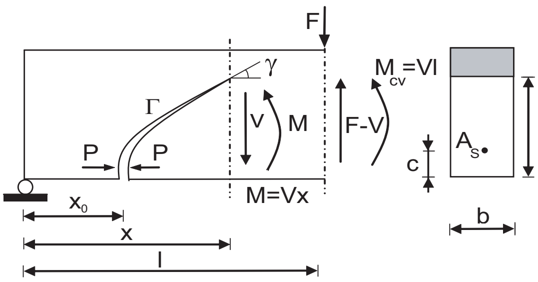

Figure 1: Cracked element.

$$\alpha(\zeta,\xi)=\begin{cases}\alpha_0 & 0\le\xi\le\zeta\\ \alpha_0+\left(\dfrac{\xi-\zeta}{1-\zeta}\right)^{\mu}(1-\alpha_0) & \zeta\le\xi\le1\end{cases}\quad(1)$$

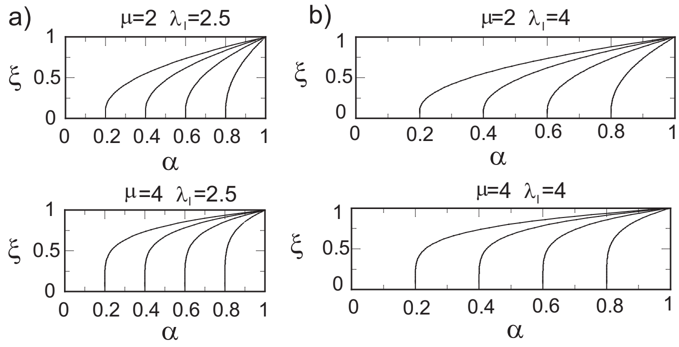

Figure 2: Crack trajectories, (a) λ_l=2.5; (b) λ_l=4.

2 MODELLING OF FLEXURAL AND SHEAR CRACKS

The *bridged crack model* can be applied for studying the propagation of a crack in a reinforced concrete beam assuming as monotonically increasing control parameter the length of the crack path. Linear Elastic Fracture Mechanics is assumed for concrete with a crack propagation condition ruled by the comparison of the stress intensity factors K_I to the concrete toughness K_{IC}. Neither closed form solution nor non-linear regressions of numerical data are available for evaluating the stress-intensity factors of the geometry given in Figure 1. Therefore, some assumptions have been made to derive suitable approximations.

The adopted model scheme is reported in Figure 1 along with the used symbols. The geometric dimensions are converted into nondimensional quantities, after dividing by the height h in the case of vertical distances and by the shear span l in the case of horizontal distances. Thus, the following nondimensional parameters are defined: let $\alpha=\frac{x}{l}$ be the nondimensional horizontal distance from the support to the crack tip, $\xi=\frac{a}{h}$ the crack depth, $\alpha_0=\frac{x_0}{l}$ the initial crack mouth position and $\zeta=\frac{c}{h}$ the reinforcement cover. All these nondimensional parameters range from 0 to 1. Additionally, let λ_l be the shear span slenderness ratio ($\lambda_l=\frac{l}{h}$).

The crack trajectory Γ is considered as formed by a first vertical segment Γ_1 from the bottom to the reinforcement layer. A second part Γ_2 is assumed being a power law with some given exponent, going from the end of the first part to the load point, Fig. 2. The crack trajectory Γ=$\Gamma_1\cup\Gamma_2$ is defined by the nondimensional function:

The constitutive relation for the reinforcement bars is assumed rigid-perfectly plastic with no upper limit to the maximum deformation. The maximum for the bridging reinforcement reaction is defined by $P_P=A_s\sigma_y$, where A_s is the reinforcement area and σ_y the minimum between yielding and sliding stress for the bars.

With reference to Figure 1, let K_I be the stress intensity factor at the crack tip. By superposition, it is given by the sum of the stress intensity factor K_{IV}, due to the bending moment associated to the shear force V, and K_{IP_γ}, due to the closing force at the reinforcement position:

$$K_I=K_{IV}-K_{IP_\gamma}\quad(2)$$

To evaluate the stress intensity factor due to the external load K_{IV}, Jenq and Shah (Jenq and Shah 1989) assumed that it can be approximated by the stress-intensity factor of a bent beam with a symmetric edge notch of depth a subjected to the bending moment corresponding to the cross section at the mouth of the crack. Here a similar approach is followed, although the variation of the bending moment at each section due to the crack path will be accounted for. Therefore:

$$K_{IV}=\frac{Vl\alpha(\zeta,\xi)}{h^{\frac{3}{2}}b}Y_M(\xi)=\frac{V}{h^{\frac{1}{2}}b}Y_V(\zeta,\xi)\lambda_l\quad(3)$$

The stress-intensity factor produced at the crack tip by the applied forces P acting at the level of the reinforcement is obtained from the case of vertical crack, K_{IP}. Several numerical analyses by boundary elements (Portela and Aliabadi 1992) have been made to get an approximation to the stress-intensity factor for different positions of the crack tip. It is observed that the stress intensity factor is a function of the angle γ, see Figure 1. Consequently, a function $\beta(\gamma)$ to approximate the variation Y_P with γ has been defined. Finally, the stress intensity factor due to the reinforcement reaction P is given by

$$K_{IP_\gamma} = \frac{P}{h^{\frac{1}{2}}b} Y_P(\zeta,\xi)\beta(\gamma) = \frac{P}{h^{\frac{1}{2}}b} Y_{P_\gamma}(\zeta,\xi) \tag{4}$$

with $\beta(\gamma) = (\frac{\gamma}{90})^{0.2}$ and γ expressed in degrees.

The functions $Y_M(\xi)$ and $Y_P(\zeta,\xi)$ are given in the stress intensity factor handbook (Okamura et al. 1975).

Let ρ be the bar reinforcement percentage defined as $\rho = \frac{A_s}{bh}$ and w the crack opening at reinforcement level. The following nondimensional parameters can be defined

$$N_P = \frac{\sigma_y h^{\frac{1}{2}}}{K_{IC}}\rho; \qquad \tilde{w} = \frac{wE}{K_{IC}h^{\frac{1}{2}}} \tag{5}$$

where N_P is the *brittleness number* defined by Carpinteri (Carpinteri 1981; 1984) and E is the Young's modulus of the material.

Substituting Eqs. (3) and (4) into Eq. (2), the following nondimensional equilibrium equation is obtained

$$\tilde{V}_F = \frac{1}{\lambda_l Y_V(\xi)}\left[1 + N_P \tilde{P} Y_{P_\gamma}(\zeta,\xi)\right] \tag{6}$$

where $\tilde{V}_F = V_F/(K_{IC}h^{\frac{1}{2}}b)$ and $\tilde{P} = P/P_P$.

The crack opening, $\tilde{w}$ at the nondimensional coordinate ζ can be determined by adding the two contributions of shear $\tilde{V}$ and bar reaction $\tilde{P}$. The nondimensional opening evaluated at the crack propagation shear V=V_F, presents the following expression:

$$\begin{aligned}\tilde{w} =& 2\lambda_l \tilde{V}_F \int_\zeta^\xi Y_V(z) Y_{P_\gamma}(\zeta,z) g(\zeta,z)\,\mathrm{d}z - \\ & 2N_P\tilde{P}\int_\zeta^\xi Y_{P_\gamma}^2(\zeta,z)g(\zeta,z)\,\mathrm{d}z\end{aligned} \tag{7}$$

where $g(\zeta,\xi)$ is the Jacobian mapping the curvilinear integral along the crack trajectory onto the interval $[0,\xi]$ (Carpinteri et al. 2006).

If the relative displacement in the cracked cross-section at the level of reinforcement is assumed to be equal to zero, up to the yielding or slippage of the reinforcement ($\tilde{w}$=0), we obtain the displacement compatibility condition that allows us to obtain the unknown force $\tilde{P}$ as a function of the applied shear $\tilde{V}$. In fact, from Eq. (7), we may define:

$$r''(\zeta,\xi) = \frac{\lambda_l \tilde{V}_F}{N_P\tilde{P}} = \frac{\int_\zeta^\xi Y_{P_\gamma}^2(\zeta,z)g(\zeta,z)\,\mathrm{d}z}{\int_\zeta^\xi Y_V(z)Y_{P_\gamma}(\zeta,z)g(\zeta,z)\,\mathrm{d}z} \tag{8}$$

If the force transmitted by the reinforcement is equal to P_P=$\sigma_y A_s$, in other words, if the reinforcement traction limit has been reached ($\tilde{V}_F$=$\tilde{V}_P$), from (6) we obtain:

$$\tilde{V}_P = \frac{1}{\lambda_l Y_V(\xi)}\Big[1 + N_P Y_{P_\gamma}(\zeta,\xi)\Big] \tag{9}$$

On the other hand, if $\tilde{V}_F < \tilde{V}_P$, the following relation holds from Eqs. (6) and (8):

$$\tilde{V}_F = \frac{1}{\lambda_l\Big[Y_V(\xi) - \dfrac{Y_{P_\gamma}(\zeta,\xi)}{r''(\zeta,\xi)}\Big]} \tag{10}$$

Therefore, according to the model, when $\tilde{V}_F < \tilde{V}_P$ the shear of crack propagation $\tilde{V}_F$ depends only on the relative crack depth ξ, and is not affected by the brittleness number N_P.

3 MODELLING CONCRETE CRUSHING

The problem of concrete crushing in the upper part of the beam is analyzed evaluating the compressive stress in the cracked element. Concrete crushing will be detected by comparing the stress σ_c to the crushing strength σ_{cu}.

The compressive stress at the upper edge of the cracked section is the sum of the contributions due to shear and reinforcement reaction:

$$\sigma_c = \sigma_c^V + \sigma_c^P \tag{11}$$

Introducing two suitable shape functions $Y_\sigma^M(\xi)$ and $Y_\sigma^P(\zeta,\xi)$ (Carpinteri et al. 2003) and letting $Y_\sigma^V(\xi) = \alpha(\zeta,\xi)Y_\sigma^M(\xi)$, the following expression is derived

$$\sigma_c = \lambda_l \frac{V}{bh} Y_\sigma^V(\xi) - \frac{P}{bh} Y_\sigma^P(\zeta,\xi) \tag{12}$$

Let $V = V_C$ be the concrete crushing load, attained when $\sigma_c = \sigma_{cu}$. In nondimensional form we may write:

$$\frac{\sigma_{cu}h^{\frac{1}{2}}}{K_{IC}} = \tilde{V}\lambda_l Y_\sigma^{V_C}(\xi) - N_P\tilde{P}Y_\sigma^P(\zeta,\xi) \tag{13}$$

Consequently, in the same way as for the steel yielding mechanism, a *brittleness number* for the crushing failure can be naturally defined:

$$N_C = \frac{\sigma_{cu}h^{\frac{1}{2}}}{K_{IC}} \tag{14}$$

so that the nondimensional shear for compression failure is given by

$$\tilde{V}_C = \frac{1}{\lambda_l Y_\sigma^V(\xi)} \left[N_C + N_P \tilde{P} Y_\sigma^P(\zeta,\xi) \right] \tag{15}$$

To eliminate the dependence on $\tilde{P}$ in (15), we may observe that, at steel yielding, it is $\tilde{P} = 1$ and therefore, from Eq. (15):

$$\tilde{V}_C = \frac{1}{\lambda_l Y_\sigma^V(\xi)} \left[N_C + N_P Y_\sigma^P(\zeta,\xi) \right] \tag{16}$$

In the same way, when $\tilde{P} < 1$, from (8) it is:

$$\tilde{V}_C = \frac{1}{\lambda_l Y_\sigma^V(\xi)} \left[N_C + \frac{Y_\sigma^P(\zeta,\xi)}{Y_V(\xi) r''(\zeta,\xi) - Y_{P_\gamma}(\zeta,\xi)} \right] \tag{17}$$

The nondimensional shear of Eqs. (16) and (17) produces, for a given crack depth ξ, the crushing stress $\sigma_c = \sigma_{cu}$ in the uppermost part of the beam. On the other hand, for equilibrium and compatibility being satisfied, only the non-dimensional shear of crack propagation, Eqs. (9) and (10), is compatible with a given crack depth ξ, so that crushing failure occurs when the crack propagation non-dimensional shear, Eqs. (9) and (10), is equal to the non-dimensional crushing shear, Eqs. (16) and (17) respectively.

For $\tilde{V}_C = \tilde{V}_F \geq \tilde{V}_P$, we have:

$$\frac{N_C + N_P Y_\sigma^P(\zeta,\xi)}{Y_\sigma^V(\xi)} = \frac{1 + N_P Y_P(\zeta,\xi)}{Y_V(\xi)} \tag{18}$$

as well as, for $\tilde{V}_C = \tilde{V}_F < \tilde{V}_P$, it is:

$$\frac{N_C + \frac{Y_\sigma^P(\zeta,\xi)}{[Y_V(\xi) r''(\zeta,\xi) - Y_{P_\gamma}(\zeta,\xi)]}}{\lambda_l Y_\sigma^V(\xi)} = \frac{1}{Y_V(\xi) - \frac{Y_{P_\gamma}(\zeta,\xi)}{r''(\zeta,\xi)}} \tag{19}$$

Equations (18) and (19) determine the points of crushing failure in in the crack depth vs. non-dimensional shear diagram.

4 FLEXURAL AND SHEAR CRACK PROPAGATION

In this section it will be shown how the value of the initial crack position α_0 affects the mechanical response of the beam and implies the stability/instability of the cracking process.

For the sake of clarity, reference is made to a real example, based on experimental results. A more detailed explanation can be found in (Carpinteri et al. 2006). The experimental test has been performed by Bosco and Carpinteri (Bosco and Carpinteri 1992), and it was labeled as B100-06. The material properties and beam geometry of this test are shown in Figure 3a.

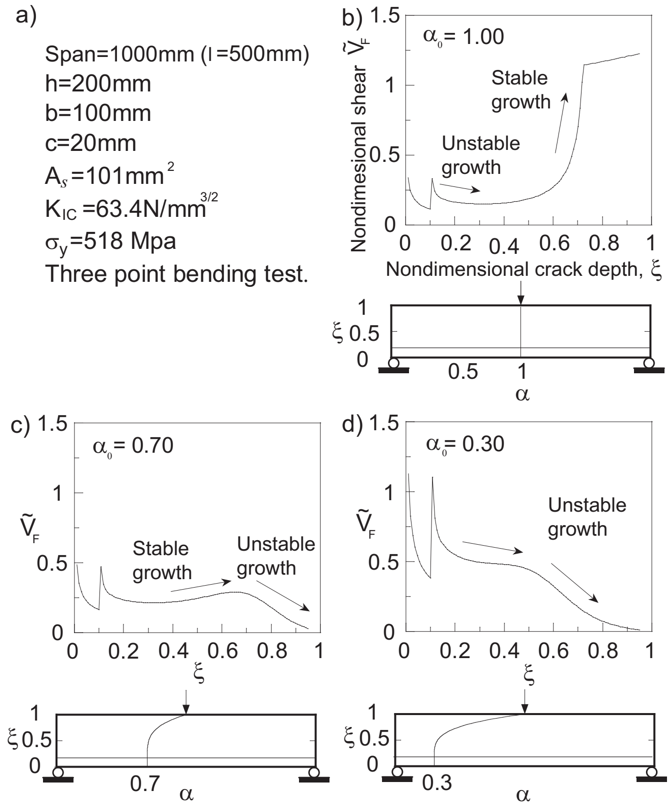

Figure 3: Nondimensional shear force vs. crack depth: (a) material properties and beam geometry; (b) initial crack position α_0=1.0; (c) initial crack position α_0=0.70; (d) initial crack position α_0=0.30.

The following nondimensional parameters characterize the simulation case: $\lambda_l = 2.5$, $\zeta = 0.1$, $N_P = 1.41$ and a 4^{th} order crack trajectory curve ($\mu = 4$) is assumed. Figures 3b-d show the nondimensional shear force vs. crack depth curves for the initial crack position α_0 in the interval [0.3, 1.0] and a sketch of the crack trajectories.

It is well-known that a crack growth may present stable or unstable behaviour. When the crack growth is stable, an increase in the crack depth requires a load increase to fulfil the model equations. On the contrary, unstable crack growth implies a load decrease. Both kinds of behavior can occur at different load levels during crack propagation, see Figures 3b, c and d.

When the initial crack position is at midspan ($\alpha_0 = 1.0$), Figure 3b, the model converges to the original *bridged crack* for beams in flexure (no shear). Immediately after the crack crosses the reinforcement, an unstable branch begins. This turns stable for a crack depth $\xi \simeq 0.3$. Then the nondimensional shear force grows until the yielding of steel takes place ($\xi \simeq 0.7$). Physically the reinforcement reaction stabilizes the initial unstable crack propagation and finally produces the steel yielding.

The second plot, Figure 3c, computed for an initial crack position $\alpha_0 = 0.70$, shows the same characteristic behaviour for low values of the crack depth, an unstable branch follows the stable branch for a crack depth value of 0.65. From this point on the crack growth is unstable leading the beam to failure. In this case, as for the flexural crack $\alpha_0 = 1.00$, the reinforcement reaction stabilizes the crack propagation for low crack depth but there is a point where the propagation becomes unstable. The change in the nature of the propagation provokes the relative maximum that is observed in Figure 3c. This change for shear crack in reinforced concrete beams without stirrups has been reported experimentally by Carmona (Carmona et al. 2006).

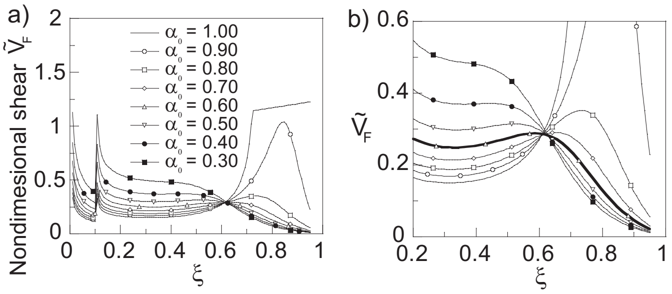

Figure 4: (a) Nondimensional shear force, $\tilde{V}_F$ vs. crack depth, ξ; (b) detail, the thick line is the curve of the minimum critical shear load.

Figure 4a shows a superposition of the plots for different initial crack positions. Observe that, neglecting the singularity at the reinforcement position, each curve presents a relative maximum with the exception of cracks near the support which are unstable during all the propagation process. The thick line in Figure 4b represents the crack having the property that its relative maximum is minimum among the maxima. This relative maximum is assumed as the shear failure load and the curve where it is located allows to determine the initial crack position as well.

The minimum in the shear force when the crack initiation position is changed along the shear span has been reported also by Niwa (Niwa 1997) in a Finite Element numerical study. Niwa fixed the shear span to depth ratio λ_l to 2.4 and assumed a linear crack path from the initiation point to the load point. The position for the crack initiation reported for the minimum shear resistance in his study was 0.62 and the nondimensional shear was 0.33. These results compare fairly well with the results of the present model.

5 CONCRETE CRUSHING FAILURE

The equations (16) and (17) reported in Section 3, give the shear producing crushing failure. But, to satisfy equilibrium and compatibility, the crushing shear must be equal to the shear of crack propagation, as expressed by (18) and (19). Therefore, the crushing points expressed by (18) and (19) can be found by intersecting the crushing curve (16) and (17) with the crack propagation curve given by (9) and (10). For a better clarity, this is done in the hypothesis that failure by crushing occurs at the central crack ($\alpha_0 = 1.0$), but the model is not restricted to this situation.

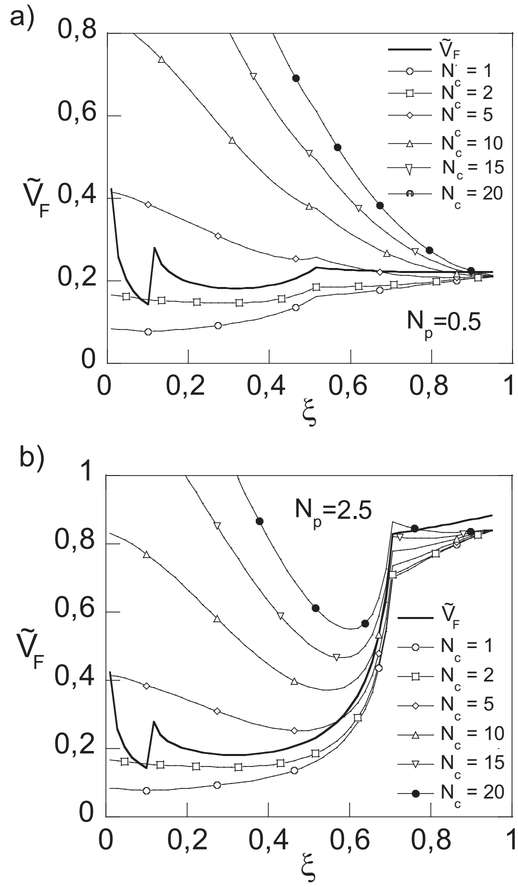

Figure 5: Influence of N_C in nondimensional shear as function of the crack depth for λ_1=2 and ζ=0.1; (a) N_P=0.5; (b) N_P=2.5.

In Fig. 5a the curve showing a discontinuity at the reinforcement position ($\xi = 0.1$) represents the nondimensional shear of crack propagation, $\tilde{V}_F$, for a vertical crack at the midspan ($\alpha_0 = 1.0$). The other family of curves represent the shear of crushing failure, $\tilde{V}_C$, for different values of N_C, Eqs. (16) and (17). As appears from Fig. 5a, if N_C is less than 2 (see the two lowest curves), the RC beam exhibits an unstable behaviour, and the fracture process cannot occur because the shear necessary for crushing is less than the shear necessary to the cracking process. For higher values of N_C the beam exhibits first yielding ($\xi \simeq 0.5$), and then crushing when the curves with varying N_C intersect the thick curve of the load vs. crack depth diagram. In this example it is therefore useless to increase the concrete strength above say

$N_C \simeq 5$ as yielding will always precede crushing and the failure mode is flexural.

In Fig. 5b the beam brittleness number N_P is varied from 0.5 to 2.5 with respect to Fig. 5a. For values of N_C smaller that 2 the beam presents the same unstable behaviour of the previous example. In contrast, for N_C higher than 4, the crushing failure occurs before yielding. As N_C is increased, the crushing collapse progressively approaches the yielding point. Only for $N_C = 20$ the yielding precedes crushing failure, as the curve for $N_C = 20$ intersects the thick curve of the cracking process only after yielding. Therefore, a variation in the brittleness number N_C can change the collapse mechanism from yielding to concrete crushing and viceversa.

6 TRANSITION BETWEEN FAILURES MODES

The proposed model covers the three fundamental failure mechanisms of RC beams: steel yielding (flexural), diagonal tension (shear) and concrete crushing. As shown in the following, the transition between the aforementioned mechanisms is ruled by the nondimensional model parameters N_P, N_C and λ_l. For the sake of clarity, first the transition from flexural to shear failure is analysed, then the transition from shear to crushing failure.

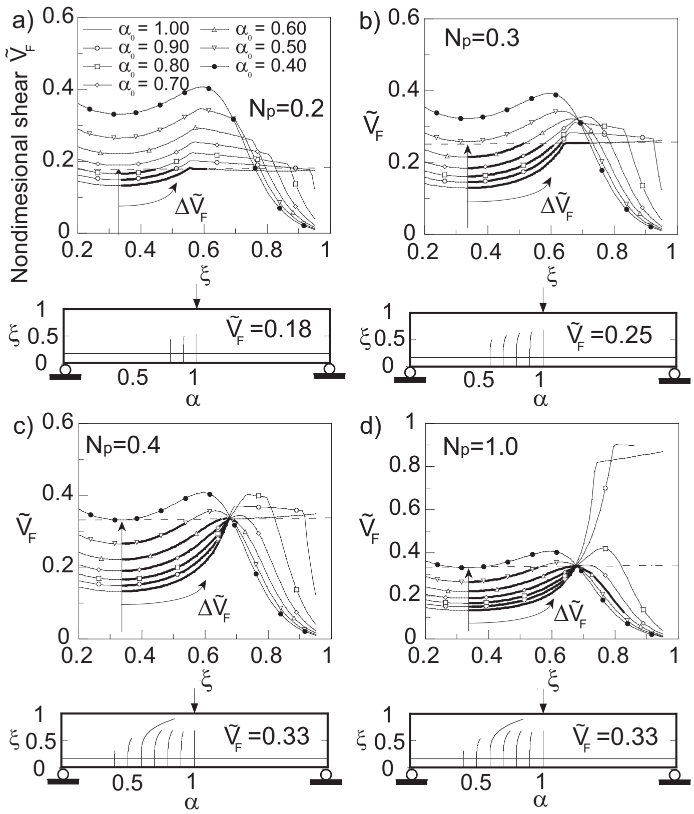

Figure 6: Transition from flexural to diagonal tension failure in RC beams as function of the governing nondimensional parameter N_P; (a) N_P=0.2; (b) N_P=0.3; (c) N_P=0.4; (d) N_P=1.0.

Figure 6 shows four $\tilde{V}_F - \xi$ curves obtained by increasing the brittleness number N_P from 0.2 to 1.0 and keeping constant all the remaining parameters ($\lambda_l = 2.5$, $\zeta = 0.1$, $\mu = 6$). A sketch illustrating the crack trajectories at failure is reported for each beam model.

In Figure 6a the model response for a brittleness number $N_P = 0.2$ is shown. When the nondimensional shear force reaches a value of 0.14 the flexural crack ($\alpha_0 = 1.00$) begins its stable growth. As the load is increased, some other neighboring cracks develop with a stable growth. The more marked lines in the plot represent the growing cracks. When the nondimensional shear force is equal to 0.18 the steel yields at the flexural crack. We assume that this value of the nondimensional shear force represents the flexural failure load. Thus the beam modeled in Figure 6a shows a flexural failure due to the yielding of the steel at the midspan crack. In the same way, when the brittleness number is increased to 0.3, the beam collapses by flexural failure at the midspan crack, although an increment in nondimensional shear force from 0.18 to 0.25 is observed. Comparing the crack pattern sketches at failure, we observe that the increment in the nondimensional shear also allows for new neighboring cracks to develop through the reinforced concrete element.

If the brittleness number is increased to 0.4, see Figure 6c, initially the cracking process is similar to the previous cases. Nevertheless, when the nondimensional shear force reaches the value 0.33, flexural and diagonal tension failure occur at the same time. In fact, as pointed out in Section 4, diagonal tension (shear) failure occurs when a shear crack develops an instability process after a stable crack growth. For higher values of the brittleness number flexural failure needs a higher nondimensional shear than diagonal tension failure, as illustrated in Fig. 6d, where the brittleness number is set to 1.0: the load required to provoke flexural collapse for the crack situated at midspan is 0.8 while the load to provoke diagonal tension failure is 0.33 for the crack in $\alpha_0 = 0.6$.

Therefore, for low values of N_P, cracks at midspan (flexural cracks) need lower nondimensional shear force to provoke flexural failure than shear cracks situated along the span to develop diagonal shear failure. As N_P is increased, the opposite case occurs: cracks along the span need lower nondimensional shear force to provoke beam collapse than the crack at midspan. Thus there is a point where the transition between these types of failure takes place.

Figure 7 shows a conceptual sketch of all the failure mode transitions in reinforced concrete elements without stirrups predicted by the model by varying the nondimensional parameters.

Based on the definition of the brittleness number

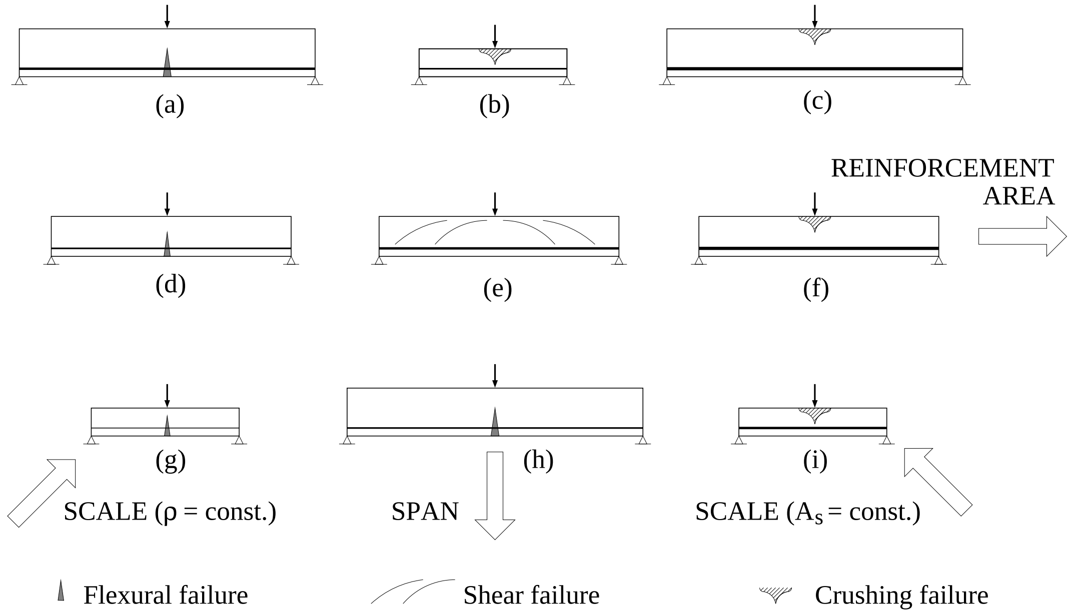

Figure 7: The global conceptual scheme illustrating failure mode transitions.

N_P, an increase in N_P can be read as:

- an increase in the reinforcement area, transition from (d) to (e);
- a decrease in the scale with constant reinforcement area, transition from (a) to (e);
- an increase in the scale with a constant reinforcement percentage, transition from (g) to (e).

When a crushing failure is considered, the behavior of the RC element is controlled by the three nondimensional parameters N_P, N_C and λ_l. As defined in Section 3, crushing failure occurs when the crushing vs. shear plot intersects the crack propagation vs. shear plot.

To simplify the explanation of the transition and for reasons of space in the present paper, a direct transition from flexural to crushing failure is illustrated, although intermediate shear failure transition can be demonstrated to exist as reported in the general scheme of Fig. 7.

In Fig. 8a the transition process is shown when N_P is varied and the rest of parameters remains constant. The nondimensional shear $\tilde{V}_F$ at yielding increases as N_P increases. At the same time, the shear for crushing failure increases, although in a smoother way. Thus the transition from flexural to crushing failure appears clearly as shown in Fig. 8b, where we can read the brittleness number in the abscissas against the nondimensional shear at failure. Two different areas are delimitated. For low values of the brittleness number failure is due to steel yielding (flexure). For $N_P \simeq 0.3$, the transition takes place and then shear for crushing failure needs a lower value compared to shear for

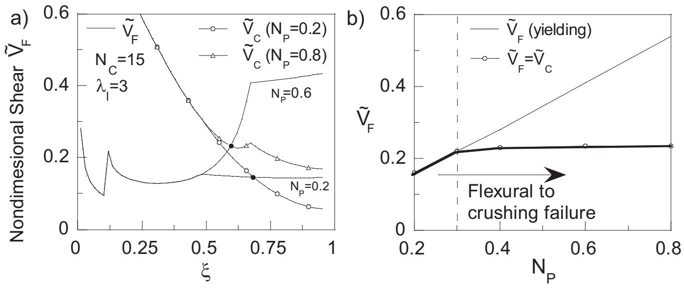

Figure 8: Transition from flexural to crushing failure in RC beams as function of governing nondimensional parameters, increment of N_P; (a) $\tilde{V}_F$-ξ curves; (b) $\tilde{V}_F$-N_P curve.

flexural failure, i.e. crushing precedes yielding. Physically this transition appears when the reinforcement ratio ρ is increased and the rest of parameters remains constant: we have the transition from (d) to (f) in the scheme of Fig. 7.

According to the scheme, another transition can be demonstrated when the beam is scaled keeping constant the reinforcement ratio ρ. Looking at the definitions of N_P and N_C, the condition of an increment in the scale can be expressed keeping constant the ratio $\frac{N_C}{N_P}$.

Finally, the transition by size effect can be demonstrated in the hypothesis that the reinforcement area A_s is constant. This condition can be expressed by considering the ratio $\frac{N_C}{N_P}$ as a linear function of the scaled beam depth $\frac{h}{h_0}$, where h_0 is a reference depth.

The conceptual scheme in Fig. 7 summarizes the failure transitions predicted by the model, from flexural crushing failure.

The transitions to crushing can take place as:

- an increase in the reinforcement area, transition from (d) to (e) and finally (f);
- an increase in the scale with constant reinforcement percentage, transition from (g) to (e) and finally (c);
- a decrease in the scale with constant reinforcement area, transition from (a) to (e) and finally (i).

In some cases, depending on material and geometrical properties, the intermediate transition through (e) may be skipped and a direct transition from yielding to crushing can be observed.

7 CONCLUSIONS

This paper presents an extension of the *bridged crack model* to analyse flexural-shear-crushing failure modes in R.C. beams. The failure mode transitions have been illustrated by varying the controlling nondimensional parameters: the brittleness numbers N_P and N_C and the slenderness λ_l. The study demonstrates that the diagonal tension failure is a consequence of unstable crack propagation. The shear failure initiation point and collapse load are determined analytically by the present model without using empirical parameters.

The model gives rational explanation to the transitions between all the failure modes and size effects in failure transitions are shown by varying the brittleness numbers, N_P and N_C.

ACKNOWLEDGEMENTS

Jacinto R. Carmona gratefully acknowledges the financial support for this research provided by the *Ministerio de Educación y Ciencia*, Spain, under grant MAT2003-00843, and by the *Ministerio de Fomento*, Spain, under grant BOE305/2003.

REFERENCES

Bosco, B. and A. Carpinteri (1992). Fracture mechanics evaluation of minimum reinforcement in concrete structures. In *Applications of Fracture Mechanics to reinforced concrete*, London, pp. 347–377. A. Carpinteri, ed., Elsevier Applied Science.

Carmona, J. R., G. Ruiz, and del Viso. J. R. (submitted 2006). Mixed-mode crack propagation through reinforced concrete. *Engineering Fracture Mechanics*.

Carpinteri, A. (1984). Stability of fracturing process in RC beams. *Journal of Structural Engineering-ASCE 110*, 544–558.

Carpinteri, A., J. R. Carmona, and G. Ventura (submitted 2006). Propagation of flexural and shear cracks through reinforced concrete beams by the bridged crack model. *Magazine of Concrete Research*.

Carpinteri, A., G. Ferro, C. Bosco, and M. Elkatieb (1999). Scale effects and transitional failure phenomena of reinforced concrete beams in flexure. In A. Carpinteri (Ed.), *Minimum Reinforcement in Concrete Members*, Volume 24 of *ESIS Publications*, pp. 1–30. Elsevier Science Ltd.

Carpinteri, A., G. Ferro, and G. Ventura (2003). Size effects on flexural response of reinforced concrete elements with a nonlinear matrix. *Engineering Fracture Mechanics 70*, 995–1013.

Carpinteri, A., G. Ferro, and G. Ventura (2004). A fracture mechanics approach to over-reinforced concrete beams. In V. Li, C. Leung, K. Willam, and S. Billington (Eds.), *Proceedings of the* 5^{th} *Fracture Mechanics of Concrete and Concrete Structures (FraMCoS-5)*, pp. 903–910.

Gustafsson, P. and A. Hillerborg (1983). Sensitivity in shear strength of longitudinally reinforced concree beams to fracture energy of concrete. *ACI Structural Journal 85*(3), 286–294.

Jenq, Y. S. and S. P. Shah (1989). Shear resistance of reinforced concrete beams - a fracture mechanics approach. In *Fracture Mechanics: Applications to Concrete*, Detroit, pp. 237–258. V. Li and Bažant, Z.P., eds., American Concrete Institute.

Niwa, J. (1997). Size effect in shear of concrete beams predicted by fracture mechanics. In *CEB Bulletin d'Information n 237 - Concrete Tension and Size Effects*, Lausanne, Switzerland, pp. 147–158. Comite Euro-International du Béton (CEB).

Okamura, H., K. Watanabe, and T. Takano (1975). Deformation and strength of cracked member under bending moment and axial force. *Engineering Fracture Mechanics 7*, 531–539.

Portela, A. and M. H. Aliabadi (1992). *Crack Growth Analysis Using Boundary Elements*. Southampton: Computational Mechanics Publications.

So, K. O. and B. Karihaloo (1993). Shear capacity of longitudinally reinforced beams - A fracture mechanics approach. *ACI Structural Journal 90*, 591–600.